CLINICAL ORAL IMPLANTS RESEARCH

Short Communication

Non-ionizing real-time ultrasonography in implant and oral surgery: A feasibility study

Hsun-Liang Chan
Hom-Lay Wang
Jeffery Brian Fowlkes
William V. Giannobile
Oliver D. Kripfgans

Authors' affiliations:
Hsun-Liang Chan, Hom-Lay Wang, William V. Giannobile, Department of Periodontics and Oral Medicine, University of Michigan School of Dentistry, Ann Arbor, MI, USA
Jeffery Brian Fowlkes, Oliver D. Kripfgans, Department of Radiology, University of Michigan Medical School, Ann Arbor, MI, USA
Jeffery Brian Fowlkes, William V. Giannobile, Department of Biomedical Engineering, College of Engineering, University of Michigan, Ann Arbor, MI, USA

Corresponding author:
Oliver D. Kripfgans, PhD
Department of Radiology and Department of Biomedical Engineering
University of Michigan
1301 Catherine St. Medical Sciences I
Room 3218D
Ann Arbor
MI 48109-5667
USA
Tel.: +734 647 0852
Fax: +734 764 8541
e-mail: oliver.kripfgans@umich.edu

Key words: alveolar ridge, anatomy, bone regeneration, cone-beam computed tomography, dental implants, ultrasonography

Abstract

Purpose: Ultrasound imaging has potential to complement radiographic imaging modalities in implant and oral surgery given that it is non-ionizing and provides instantaneous images of anatomical structures. For application in oral and dental imaging, its qualities are dependent on its ability to accurately capture these complex structures. Therefore, the aim of this feasibility study was to investigate ultrasound to image soft tissue, hard tissue surface topography and specific vital structures.

Material and methods: A clinical ultrasound scanner, paired with two 14-MHz transducers of different sizes (one for extraoral and the other for intraoral scans), was used to scan the following structures on a fresh cadaver: (i) the facial bone surface and soft tissue of maxillary anterior teeth, (ii) the greater palatine foramen; (iii) the mental foramen and (iv) the lingual nerve. Multiple measurements relevant to these structures were made on the ultrasound images and compared to those on cone-beam computed tomography (CBCT) scans and/or direct measurements.

Results: Ultrasound imaging could delineate hard tissue surfaces, including enamel, root dentin and bone as well as soft tissue with high resolution (110 μm wavelength). The greater palatine foramen, mental foramen and lingual nerve were clearly shown in ultrasound images. Merging ultrasound and CBCT images demonstrated overall spatial accuracy of ultrasound images, which was corroborated by data gathered from direct measurements.

Conclusion: For the first time, this study provides proof-of-concept evidence that ultrasound can be a real-time and non-invasive alternative for the evaluation of oral and dental anatomical structures relevant for implant and oral surgery.

Understanding the location, size, shape and spatial relationships of dental and oral structures is essential for clinicians to plan and execute surgeries. During the past decade, cone-beam computed tomography (CBCT), owing to its ability to replicate anatomy accurately in three dimensions, has greatly supplemented the use of two-dimensional (2D) conventional dental radiographs (Loubele et al. 2007; Ludlow et al. 2007; Chan et al. 2010b). Although a single CBCT scan delivers low-dose radiation, repeated scans on the same patient are not advisable (e.g., during a surgery to avoid injuring vital structures) (Horner et al. 2009). Furthermore, CBCT is not applicable for evaluating peri-implant structures due to beam hardening and scattering artifacts (Gonzalez-Martin et al. 2015; Kuhl et al. 2015).

Non-ionizing, real-time and less expensive ultrasound imaging is extensively used in quantitative medical diagnostics for evaluating fetal tissue dimensions for several decades (Hadlock et al. 1991). The ultrasound scanner transmits high-frequency ultrasonic pulses, between 1 and 20 MHz in general, into the region of interest with a transducer that both transmits and receives such pulses. Based on time of travel of ultrasound pulses and their received pressure amplitudes, the scanner displays a grayscale image depicting the tissue distance from the ultrasound transducer and the tissue echogenicity (reflectivity) with respect to the original pulses. Although not able to reasonably penetrate bone with the current diagnostic imaging frequencies, ultrasound can delineate bone surface explicitly, providing an adequate

Date:
Accepted 24 January 2016

To cite this article:
Chan H-L, Wang H-L, Fowlkes JB, Giannobile WV, Kripfgans OD. Non-ionizing real-time ultrasonography in implant and oral surgery: a feasibility study.
Clin. Oral Impl. Res. **28**, 2017, 341–347
doi: 10.1111/clr.12805

morphological depiction of the bone (Backhaus et al. 2001; Cardinal et al. 2001; Barratt et al. 2006; Blankstein 2011). Because of this unique feature, it has been gradually adapted in orthopedics for diagnosing bone fracture and bone diseases that erode/invade bony surfaces (Backhaus et al. 2001; Cardinal et al. 2001; Barratt et al. 2006; Blankstein 2011).

In Dentistry, ultrasound imaging is mainly used as a research tool for dental diagnosis, such as evaluating tooth structures (Bozkurt et al. 2005; Culjat et al. 2003; Hughes et al. 2009; Slak et al. 2011), soft tissue lesions (Chandak et al. 2011; Friedrich et al. 2010; Pallagatti et al. 2012; Wakasugi-Sato et al. 2010; Yamamoto et al. 2011), peri-apical lesions (Cotti et al. 2002, 2003; Gundappa et al. 2006; Rajendran & Sundaresan 2007; Aggarwal et al. 2008), periodontal bony defects (Tsiolis et al. 2003; Mahmoud et al. 2010; Chifor et al. 2011), gingival thickness (Muller & Kononen 2005; Muller et al. 2007) and for implant-related applications (Culjat et al. 2008; Machtei et al. 2010). However, it can potentially become a chair-side imaging modality during implant and oral surgery, in addition to the use of other radiographs because it reveals unprecedented soft tissue contrast and hard tissue surface topography in cross-sectional views. Recent technological advances have resulted in smaller transducers, which can accelerate the acceptance of ultrasound imaging in the dental community for intraoral applications. Therefore, this proof-of-principle study aimed to determine whether ultrasound can image some specific oral and dental landmarks that are important for performing oral surgical and implant-related procedures.

Material and methods

This is a non-regulated study, as determined by the University of Michigan Institutional Review Board (Study ID: HUM00107975).

Specimen acquisition and ultrasound equipment

A fresh 85-year-old male cadaveric head was used in this study. The specimen was kept frozen at -20°C until the initiation of the experiment. One examiner (OK), who specializes in ultrasound imaging, controlled the scanner, and one periodontist (HC) guided the ultrasound probe. A clinical ultrasound scanner (ZS3, Zonare, Mountain View CA, USA) was used and paired with a 14-MHz linear array transducer (L14-5w) for extraoral scans and a 14-MHz intraoperative array transducer (L14-5sp) for intraoral scans (Fig. 1). To obtain well-resolved bone edges, a specific function on the scanner, named spatial compounding was selected. Suitable signal-to-noise, as anticipated in oral soft tissue imaging, allowed for the selection of a dynamic range of 80 dB for large soft tissue contrast. Acoustic coupling for conduction of sound waves was achieved with the application of ultrasound gel and the use of gel-based stand-off pads. The anatomies of interest were (i) the facial alveolar bone surface and mucosa of maxillary anterior teeth, (ii) the greater palatine foramen, (iii) the mental foramen and (iv) the lingual nerve.

Placement of the transducer

1. Scans of anterior maxilla: The transducer was placed at the midline of the teeth mesiodistally, approximately following their long axes. Both extraoral and intraoral scans were performed.
2. Scans of the greater palatine foramen: The transducer was placed at the intersection of the palatine and alveolar process of the maxillary bone, slightly distal to the 2nd molar, where the foramen is most commonly located (Fu et al. 2011). The transducer was then moved anteroposteriorly and apicocoronally in small increments until the foramen could be seen.
3. Scans of the mental foramen: The transducer was placed extraorally with its long axis approximately parallel to that of the 1st and 2nd premolars. The transducer was then moved anteroposteriorly and tilted faciolingually until the foramen and facial surface of the tooth and alveolar bone could be clearly imaged.
4. Scans of the lingual nerve: The transducer was first placed at the lingual side of the mandibular 2nd molar at the level of the alveolar crest apicocoronally (Chan

Fig. 1. Ultrasound scanner and transducers used in this study. The scanner is equipped with a display, a control panel and a central processing unit. Two transducers with frequency of 14 MHz were used for extraoral and intraoral scans, respectively.

et al. 2010a). The transducer was then moved along the surface of the lingual mucosa until the nerve was revealed in the image.

Images were saved in standard clinical Digital Imaging and Communications for Medicine (DICOM) format. The ultrasound image contrast was optimized, a process called windowing, using imaging software (ImageJ, National Institutes of Health, Bethesda, MD, USA) for comparison with CBCT. The threshold was selected so that the edge of the structure, for example, hard tissue surfaces with strong ultrasound echoes, was sharpened on the image for better identification.

CBCT scanning

The specimen was scanned by an experienced operator using a CBCT scanner (3D Accuitomo 170, JMorita, Japan), with scanning parameters of 120 kVp, 18.66 mAs, scan time of 20 s and resolution of 200 μm. A cheek retractor and cotton rolls were used to delineate facial mucosa from gingiva/alveolar mucosa. The captured CBCT scans were three-dimensionally reconstructed with the built-in software and saved in DICOM format, and subsequently exported to commercially available software (Invivo5, Anatomage Dental, San Jose, CA, USA). The cross-sectional slices corresponding to the ultrasound scan images were saved and compared to the ultrasound images.

Preparation of gross anatomy

After ultrasound and CBCT scans were performed, a full-thickness facial flap was raised to reveal the facial bone surface in the maxillary anterior region (Fig. 2) and the mental foramen in the mandibular premolar region. Cross sections of the anterior teeth along with their surrounding tissues were prepared with a powered handsaw and photographed. Soft tissue overlying the greater palatine foramen was excised to visualize and measure the foramen. The lingual was dissected following a technique described in a previously published article (Chan et al. 2010a) for a direct measurement of its dimension.

Quantitative analysis

The following linear measurements were made by one calibrated examiner (HC) on ultrasound images and compared to those on CBCT images and/or direct measurements on the specimen: (1) the distance between the bone crest and the cementoenamel junction (CEJ) and (2) the mucosa thickness at 5 mm from the CEJ on the facial side of all maxillary anterior teeth, (3) the mesiodistal diameter of the greater palatine foramen, (4) the mucosal thickness over the foramen, (5) the distance between the superior border of the mental foramen and the alveolar crest, (6) the diameter of the mental foramen and (7) the diameter of the lingual nerve. Mucosal thickness on the cadaver was measured with a caliper (IWANSON spring caliper for wax, Hu-Friedy, Chicago, IL, USA) accurate to 0.1 mm. Other direct measurements were made with a periodontal probe (the University of North Carolina (UNC) Probe, Hu-Friedy, Chicago, IL, USA) accurate to 1 mm. Mean values of measurements (1) and (2) were calculated by averaging the readings from the six maxillary anterior teeth.

Results

Results of the measurements are summarized in the Table 1. The mean distance between alveolar crest and cementoenamel junction measured by ultrasound is 4.3 ± 1.1 mm, compared to 4.6 ± 0.4 mm and 4.1 ± 0.9 mm for CBCT and direct readings, respectively. The mean anterior mucosal thickness is 0.3 ± 0.1 mm on ultrasound images; while the corresponding CBCT and direct readings are 0.5 ± 0.1 mm and 0.3 ± 0.1 mm, respectively. Anatomical findings on 2D ultrasound images in relation to CT images and gross anatomy are described below.

Maxillary anterior region with intraoral ultrasound scan

The enamel surface closer to the CEJ, the root surface between the CEJ and the alveolar crest, alveolar bone surface, and the overlying mucosa could be identified (Fig. 3). The enamel, root dentin and bone surface are hyperechoic because of strong sound reflection from these surfaces. The shadow under the hyperechoic tooth and bone surface is an artifact due to ultrasound's strong reflection on hard surfaces. The multiple parallel white lines under the enamel surface (Fig. 3) may be related to the internal structural layers of the tooth, yet their spatial distance is not

Fig. 2. Frontal view of the maxillary anterior teeth before and after full-thickness flap elevation. The buccal plate is thin. The distance between CEJ to the bone crest is 4.1 ± 0.9 mm. The mucosal thickness at 5 mm apical to the CEJ is 0.3 ± 0.1 mm.

Table 1. **Comparisons between ultrasound, cone-beam computed tomography and direct measurements**

Anatomical location	Maxilla				Mandible		
	Anterior		Posterior		Posterior		
Parameter (mm)	BC-CEJ Mean ± SD (Median)	MT Mean ± SD (Median)	GPF-d	MT-GPF	MF-d	AC-MF	LN-d
Ultrasound	4.3 ± 1.1 (4.1)	0.3 ± 0.1 (0.3)	5.8	6.3	3.8	16.4	2.3
CBCT	4.6 ± 0.4 (4.6)	0.5 ± 0.1 (0.5)	6.7	6.5	3.7	16.9	N/A
Direct	4.1 ± 0.9 (4.0)	0.3 ± 0.1 (0.3)	N/A	N/A	4.1	16.0	2.5

CBCT, cone-beam computed tomography measurements; Direct, direct measurements; BC-CEJ, the distance between alveolar crest and cementoenamel junction; MT, mucosal thickness at 5 mm apical to CEJ; GPF-d, diameter of the greater palatine foramen; MT-GPF; mucosal thickness over greater palatine foramen; MF-d, diameter of mental foramen; AC-MF, the distance between alveolar crest and MF; LN-d, diameter of lingual N. N/A, not assessed (N = 6 for anterior specimens and 1 each for posterior specimens).

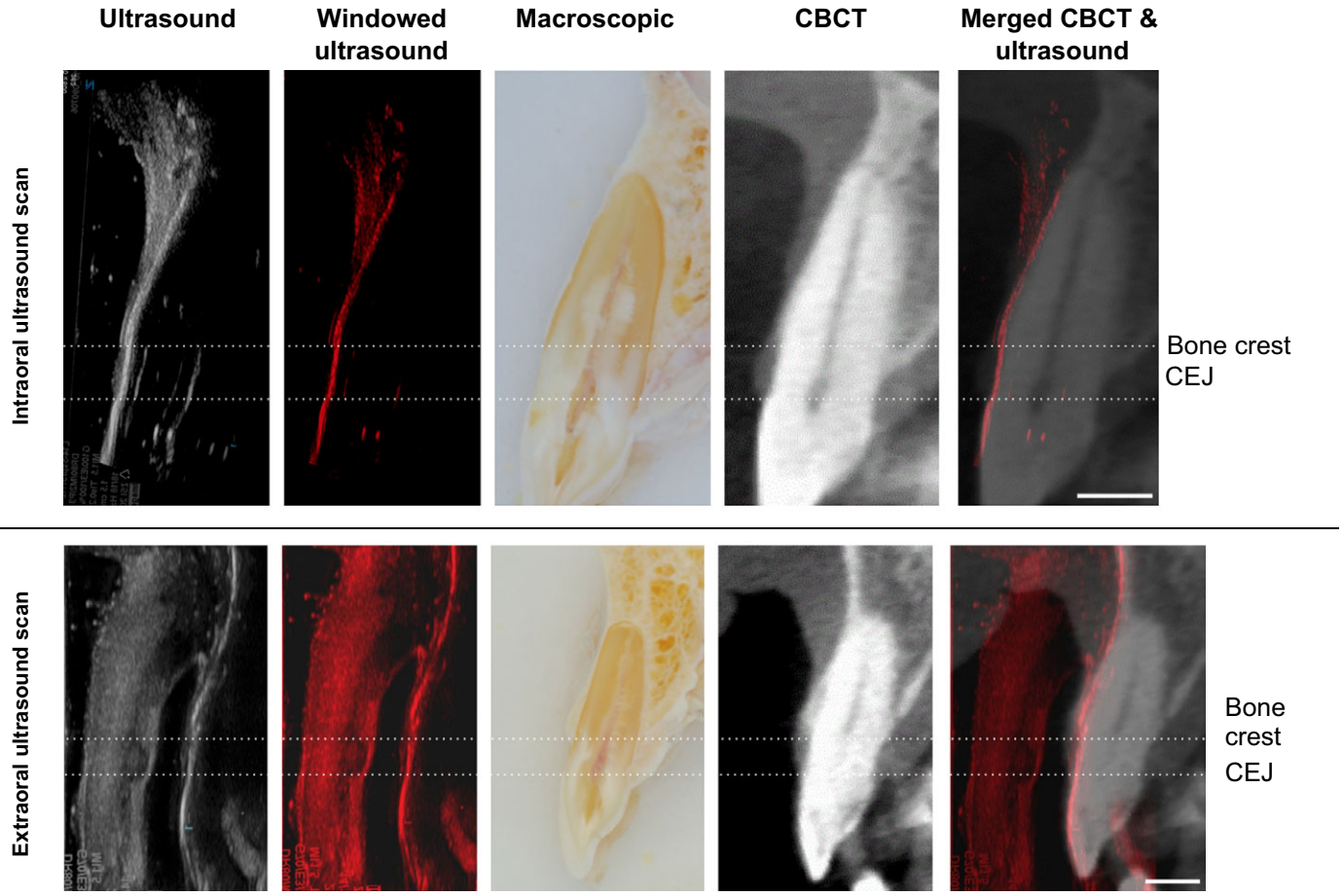

Fig. 3. Intraoral and extraoral ultrasound scans of maxillary anterior teeth. The colored and windowed ultrasound image is to highlight hard tissue surfaces that are hyperechoic. A merged image is to show match of the spatial relationship of dental anatomy. On the ultrasound image, the surfaces of enamel, root dentin and alveolar bone are clearly delineated. Additionally, the soft tissue layer, including alveolar mucosa, submucosa and muscle layers, can be seen. On the extraoral ultrasound image, the surfaces of enamel, root dentin and alveolar bone are also clearly delineated. The labial concavity apical to the root apex can be seen with this extraoral scan. Additionally, the soft tissue layer, including the lip, alveolar mucosa, submucosa and muscle layers, can be seen. (CEJ: cementoenamel junction) (Scale bar = 5 mm).

calibrated due to the higher speed of sound in the enamel (5500 m/s) and dentine (3600 m/s) when compared to the soft tissue (1540 m/s). The size and spatial relationships of the aforementioned external structures are aligned with those in CBCT images (Fig. 3 and Table 1).

Maxillary anterior region with extraoral scan

In addition to depicting structures in the vicinity to the tooth that could also be seen in intraoral scans, extraoral scans can reveal the vestibular depth and different muscle layers, orientations and their insertions to the maxilla within the lip (Fig. 3). The facial concavity of the maxilla is shown in the ultrasound scan.

Greater palatine foramen, mental foramen and lingual nerve

The greater palatine foramen is characterized by a discontinuity of the hyperechoic bone surfaces (Fig. 4). The greater palatine bundle could be visualized in the canal. Like the greater palatine foramen, the mental foramen is a discontinuity of the facial mandibular bone surface (Fig. 4). Additionally, this extraoral ultrasound scan displayed the depth of the vestibule, gingiva/mucosa around the premolar, enamel, root and bone surfaces, the buccinators m. and the depressor muscles of the mandible. The lingual nerve was presented as a hyperechoic structure in the lingual submucosa by the cortical surface of the mandible (Fig. 4). As it extends upwards in the parapharyngeal space, its course was shown as a hypoechoic ovoid.

Discussion

This pilot study demonstrates the feasibility of ultrasound to evaluate multiple important oral and dental anatomical structures. Tissue biotype is considered an important determinant to manifestation/treatment outcomes of periodontal diseases (Fu et al. 2010; Chao et al. 2015), and esthetic risk of dental/implant therapy (Lin et al. 2014). Various methods have thus been developed to evaluate tissue biotype, with probing and visual assessment being the most commonly applied methods (Kan et al. 2010). Ultrasound has been used for this purpose with high accuracy (Muller & Kononen 2005; Muller et al. 2007). However, the scanners used in the literature often only display readings of mucosal thickness, not images (Muller & Kononen 2005; Muller et al. 2007). Displaying images is advantageous because it is both more visual and more informative for the purpose of planning surgeries and comparing treatment outcomes. In addition to providing static measurements, ultrasound images might show blood flow and elasticity of oral mucosa, which could prove critical for designing flaps and determining the healing potential of bone/soft tissue regenerative procedures (Chao et al. 2015).

This pilot study demonstrates the feasibility of ultrasound for identifying the greater

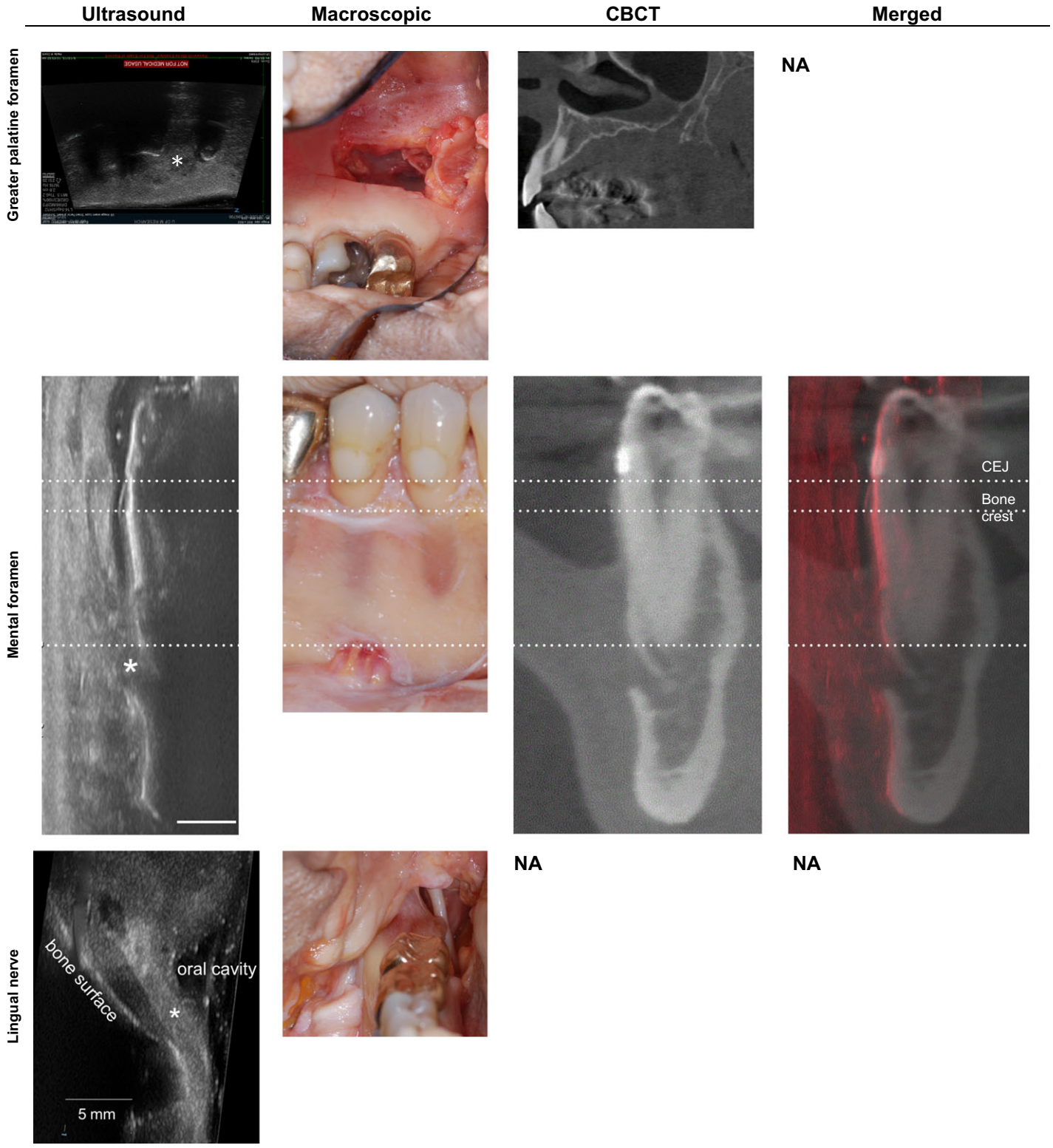

Fig. 4. An image composite including images of the greater palatine foramen, the mental foramen and the lingual nerve. The greater palatine foramen and the mental foramen are shown in the ultrasound image as a discontinuity of the bone surface. The ultrasound image including the mental foramen also presents a clear delineation of the surface of enamel, root dentin, alveolar bone and the mucosal layer. The merged images demonstrate an overall spatial registration of ultrasound and CT image, suggesting the accuracy of ultrasound images for mapping the surface topography of oral anatomy. The lingual nerve (asterisk) is shown as a hyperechoic structure lying next to the lingual side of the mandible, shown as a hyperechoic line. (CEJ, cementoenamel junction; NA, not available) (Scale bar = 5 mm).

palatine foramen, mental foramen and lingual nerve. Therefore, ultrasound-guided anesthesia, which has been gaining popularity medically (Neal et al. 2010), might be useful for facilitating block anesthesia of these nerves more efficiently. Current techniques for applying local anesthesia use anatomical landmarks to locate targeted sensory nerves. Anatomical variation of nerve

location can result in ineffective anesthesia. Multiple attempts to apply local anesthetic agent might increase systemic toxicity. The greater palatine nerve might be mislocated by up to 4 mm in a cadaver study because of variations in the vault height and the thickness of palatal mucosa (Fu et al. 2011). The mental foramen, although often palpable clinically, could be misdiagnosed, especially in patients with severe alveolar ridge resorption. Additionally, ultrasound might reduce the incidence of injuring these important structures during surgery, especially in a minimally invasive surgery.

This project was not designed to quantitatively validate the accuracy of ultrasound images; nevertheless, the size and spatial relationships of the anatomies on ultrasound images agreed with CBCT scans and direct measurements. The facial alveolar crest of the maxillary anterior teeth is, on average, approximately 4 mm apical to the CEJ, measured with the three methods. The mean facial mucosal thickness is in a range of 0.3–0.5 mm for all three methods. Future studies with a larger sample size are underway to compare these measurements between ultrasound and CT images and the direct measurements for quantitative validation. Furthermore, the accuracy of ultrasound to determine other clinically relevant parameters, for example, the degree of facial concavity of the maxilla (Chan et al. 2014) and the buccal plate thickness (Fu et al. 2010), should also be evaluated.

The limitation of ultrasound imaging is that structures within bone could not be seen, such as the inferior alveolar nerve. Therefore, some types of radiographic image would still likely be required. Additionally, a medium is required for sound transmission. Challenges of widely applying ultrasound imaging to oral surgery are (i) efforts to develop a system optimized for oral scanning, (ii) equipment costs, (iii) a learning curve for surgeon to read and interpret ultrasound data, (iv) openness of ultrasound equipment manufacturers to this new indication and (v) acceptance of this novel modality to the dental community.

Conclusions

This study demonstrates the feasibility of ultrasound for imaging oral soft tissue, hard tissue surfaces and specific vital structures. Therefore, ultrasound has significant potential to aid surgeons in "visualizing" oral structures during minimally invasive surgery and guide local anesthesia for difficult cases. Validation of this imaging modality in a more extended population with different bone and soft tissue densities will be required before implementation to clinical practice.

Acknowledgements: The authors would like to thank Mr. Dean Mueller, Coordinator of the Anatomical Donations Program for preparing the specimen, Dr. Erika Benavides, DDS, PhD, Clinical Associate Professor and Mrs. Earlene Landis for providing CBCT services, Mrs. Jill Goff, Senior Manager of Research Development Support, Mrs. Karen Gardner, Administrative Assistant Intermediate, and Dr. Jia-Hui Fu, Assistant Professor, National University of Singapore, for editing the manuscript. We would also like to acknowledge Zonare Inc. for kindly providing us with the L14-5sp ultrasound probe.

Disclaimers

The authors do not have any financial interests, either directly or indirectly, in the products or information listed in the study. The study was supported by a pilot grant (UL1TR000433) from the Michigan Institute for Clinical & Health Research (MICHR) and the University of Michigan Periodontal Graduate Student Research Fund.

References

Aggarwal, V., Logani, A. & Shah, N. (2008) The evaluation of computed tomography scans and ultrasounds in the differential diagnosis of periapical lesions. *Journal of Endodontics* **34**: 1312–1315.

Backhaus, M., Burmester, G.R., Gerber, T., Grassi, W., Machold, K.P., Swen, W.A., Wakefield, R.J. & Manger, B. (2001) Guidelines for musculoskeletal ultrasound in rheumatology. *Annuals of Rheumatic Disease* **60**: 641–649.

Barratt, D.C., Penney, G.P., Chan, C.S., Slomczykowski, M., Carter, T.J., Edwards, P.J. & Hawkes, D.J. (2006) Self-calibrating 3d-ultrasound-based bone registration for minimally invasive orthopedic surgery. *IEEE Transactions on Medical Imaging* **25**: 312–323.

Blankstein, A. (2011) Ultrasound in the diagnosis of clinical orthopedics: The orthopedic stethoscope. *World Journal of Orthopedics* **2**: 13–24.

Bozkurt, F.O., Tagtekin, D.A., Hayran, O., Stookey, G.K. & Yanikoglu, F.C. (2005) Accuracy of ultrasound measurement of progressive change in occlusal enamel thickness. *Oral Surgery Oral Medicine Oral Pathology Oral Radiology and Endodontology* **99**: 101–105.

Cardinal, E., Bureau, N.J., Aubin, B. & Chhem, R.K. (2001) Role of ultrasound in musculoskeletal infections. *Radiologic Clinics of North America* **39**: 191–201.

Chan, H.L., Garaicoa-Pazmino, C., Suarez, F., Monje, A., Benavides, E., Oh, T.J. & Wang, H.L. (2014) Incidence of implant buccal plate fenestration in the esthetic zone: a cone beam computed tomography study. *International Journal of Oral Maxillofacial Implants* **29**: 171–177.

Chan, H.L., Leong, D.J., Fu, J.H., Yeh, C.Y., Tatarakis, N. & Wang, H.L. (2010a) The significance of the lingual nerve during periodontal/implant surgery. *Journal of Periodontology* **81**: 372–377.

Chan, H.L., Misch, K. & Wang, H.L. (2010b) Dental imaging in implant treatment planning. *Implant Dentistry* **19**: 288–298.

Chandak, R., Degwekar, S., Bhowte, R.R., Motwani, M., Banode, P., Chandak, M. & Rawlani, S. (2011) An evaluation of efficacy of ultrasonography in the diagnosis of head and neck swellings. *Dentomaxillofacial Radiology* **40**: 213–221.

Chao, Y.C., Chang, P.C., Fu, J.H., Wang, H.L. & Chan, H.L. (2015) Surgical site assessment for soft tissue management in ridge augmentation procedures. *International Journal of Periodontics and Restorative Dentistry* **35**: e75–e83.

Chifor, R., Hedesiu, M., Bolfa, P., Catoi, C., Crisan, M., Serbanescu, A., Badea, A.F., Moga, I. & Badea, M.E. (2011) The evaluation of 20 mhz ultrasonography, computed tomography scans as compared to direct microscopy for periodontal system assessment. *Medical Ultrasonography* **13**: 120–126.

Cotti, E., Campisi, G., Ambu, R. & Dettori, C. (2003) Ultrasound real-time imaging in the differential diagnosis of periapical lesions. *International Endodontic Journal* **36**: 556–563.

Cotti, E., Campisi, G., Garau, V. & Puddu, G. (2002) A new technique for the study of periapical bone lesions: ultrasound real time imaging. *International Endodontic Journal* **35**: 148–152.

Culjat, M.O., Choi, M., Singh, R.S., Grundfest, W.S., Brown, E.R. & White, S.N. (2008) Ultrasound detection of submerged dental implants through soft tissue in a porcine model. *Journal of Prosthetic Dentistry* **99**: 218–224.

Culjat, M., Singh, R.S., Yoon, D.C. & Brown, E.R. (2003) Imaging of human tooth enamel using ultrasound. *IEEE Transactions on Medical Imaging* **22**: 526–529.

Friedrich, R.E., Zustin, J. & Scheuer, H.A. (2010) Adenomatoid odontogenic tumour of the mandible. *Anticancer Research* **30**: 1787–1792.

Fu, J.H., Hasso, D.G., Yeh, C.Y., Leong, D.J., Chan, H.L. & Wang, H.L. (2011) The accuracy of identifying the greater palatine neurovascular bundle: a

cadaver study. *Journal of Periodontology* **82**: 1000–1006.

Fu, J.H., Yeh, C.Y., Chan, H.L., Tatarakis, N., Leong, D.J. & Wang, H.L. (2010) Tissue biotype and its relation to the underlying bone morphology. *Journal of Periodontology* **81**: 569–574.

Gonzalez-Martin, O., Oteo, C., Ortega, R., Alandez, J., Sanz, M. & Veltri, M. (2015) Evaluation of peri-implant buccal bone by computed tomography: an experimental study. *Clinical Oral Implants Research*, doi: 10.1111/clr.12663.

Gundappa, M., Ng, S.Y. & Whaites, E.J. (2006) Comparison of ultrasound, digital and conventional radiography in differentiating periapical lesions. *Dentomaxillofacial Radiology* **35**: 326–333.

Hadlock, F.P., Harrist, R.B. & Martinez-Poyer, J. (1991) In utero analysis of fetal growth: a sonographic weight standard. *Radiology* **181**: 129–133.

Horner, K., Islam, M., Flygare, L., Tsiklakis, K. & Whaites, E. (2009) Basic principles for use of dental cone beam computed tomography: consensus guidelines of the european academy of dental and maxillofacial radiology. *Dentomaxillofac Radiology* **38**: 187–195.

Hughes, D.A., Girkin, J.M., Poland, S., Longbottom, C., Button, T.W., Elgoyhen, J., Hughes, H., Meggs, C. & Cochran, S. (2009) Investigation of dental samples using a 35mhz focussed ultrasound piezocomposite transducer. *Ultrasonics* **49**: 212–218.

Kan, J.Y., Morimoto, T., Rungcharassaeng, K., Roe, P. & Smith, D.H. (2010) Gingival biotype assessment in the esthetic zone: visual versus direct measurement. *International Journal of Periodontics and Restorative Dentistry* **30**: 237–243.

Kuhl, S., Zurcher, S., Zitzmann, N.U., Filippi, A., Payer, M. & Dagassan-Berndt, D. (2015) Detection of peri-implant bone defects with different radiographic techniques – a human cadaver study. *Clinical Oral Implants Research* doi: 10.1111/clr.12619.

Lin, G.H., Chan, H.L. & Wang, H.L. (2014) Effects of currently available surgical and restorative interventions on reducing midfacial mucosal recession of immediately placed single-tooth implants: a systematic review. *Journal of Periodontology* **85**: 92–102.

Loubele, M., Guerrero, M.E., Jacobs, R., Suetens, P. & van Steenberghe, D. (2007) A comparison of jaw dimensional and quality assessments of bone characteristics with cone-beam ct, spiral tomography, and multi-slice spiral ct. *International Journal of Oral and Maxillofacial Implants* **22**: 446–454.

Ludlow, J.B., Laster, W.S., See, M., Bailey, L.J. & Hershey, H.G. (2007) Accuracy of measurements of mandibular anatomy in cone beam computed tomography images. *Oral Surgery Oral Medicine Oral Pathology Oral Radiology and Endodontology* **103**: 534–542.

Machtei, E.E., Zigdon, H., Levin, L. & Peled, M. (2010) Novel ultrasonic device to measure the distance from the bottom of the osteotome to various anatomic landmarks. *Journal of Periodontology* **81**: 1051–1055.

Mahmoud, A.M., Ngan, P., Crout, R. & Mukdadi, O.M. (2010) High-resolution 3d ultrasound jawbone surface imaging for diagnosis of periodontal bony defects: an in vitro study. *Annual of Biomedical Engineering* **38**: 3409–3422.

Muller, H.P., Barrieshi-Nusair, K.M. & Kononen, E. (2007) Repeatability of ultrasonic determination of gingival thickness. *Clinical Oral Investigation* **11**: 439–442.

Muller, H.P. & Kononen, E. (2005) Variance components of gingival thickness. *Journal of Periodontal Research* **40**: 239–244.

Neal, J.M., Brull, R., Chan, V.W., Grant, S.A., Horn, J.L., Liu, S.S., McCartney, C.J., Narouze, S.N., Perlas, A., Salinas, F.V., Sites, B.D. & Tsui, B.C. (2010) The asra evidence-based medicine assessment of ultrasound-guided regional anesthesia and pain medicine: executive summary. *Regional Anesthesia and Pain Medicine* **35**: S1–S9.

Pallagatti, S., Sheikh, S., Puri, N., Mittal, A. & Singh, B. (2012) To evaluate the efficacy of ultrasonography compared to clinical diagnosis, radiography and histopathological findings in the diagnosis of maxillofacial swellings. *European Journal of Radiology* **81**: 1821–1827.

Rajendran, N. & Sundaresan, B. (2007) Efficacy of ultrasound and color power doppler as a monitoring tool in the healing of endodontic periapical lesions. *Journal of Endodontics* **33**: 181–186.

Slak, B., Ambroziak, A., Strumban, E. & Maev, R.G. (2011) Enamel thickness measurement with a high frequency ultrasonic transducer-based hand-held probe for potential application in the dental veneer placing procedure. *Acta of Bioengineering and Biomechanics* **13**: 65–70.

Tsiolis, F.I., Needleman, I.G. & Griffiths, G.S. (2003) Periodontal ultrasonography. *Journal of Clinical Periodontology* **30**: 849–854.

Wakasugi-Sato, N., Kodama, M., Matsuo, K., Yamamoto, N., Oda, M., Ishikawa, A., Tanaka, T., Seta, Y., Habu, M., Kokuryo, S., Ichimiya, H., Miyamoto, I., Kito, S., Matsumoto-Takeda, S., Wakasugi, T., Yamashita, Y., Yoshioka, I., Takahashi, T., Tominaga, K. & Morimoto, Y. (2010) Advanced clinical usefulness of ultrasonography for diseases in oral and maxillofacial regions. *International Journal of Dentistry* **2010**: 639382.

Yamamoto, N., Yamashita, Y., Tanaka, T., Ishikawa, A., Kito, S., Wakasugi-Sato, N., Matsumoto-Takeda, S., Oda, M., Miyamoto, I., Yamauchi, K., Shiiba, S., Seta, Y., Matsuo, K., Koga, H., Takahashi, T. & Morimoto, Y. (2011) Diagnostic significance of characteristic findings on ultrasonography for the stitch abscess after surgery in patients with oral squamous cell carcinoma. *Oral Oncology* **47**: 163–169.